Microstructured Cantilever Probe on Optical Fiber Tip for Microforce Sensor

Famei WANG[1,2], Changrui LIAO[1,2*], Mengqiang ZOU[1,2], Dejun LIU[1,2], Haoqiang HUANG[1,2], Chao LIU[3], and Yiping WANG[1,2]

[1]*Shenzhen Key Laboratory of Ultrafast Laser Micro/Nano Manufacturing, Key Laboratory of Optoelectronic Devices and Systems of Ministry of Education/Guangdong Province, College of Physics and Optoelectronic Engineering, Shenzhen University, Shenzhen 518060, China*

[2]*Shenzhen Key Laboratory of Photonic Devices and Sensing Systems for Internet of Things, Guangdong and Hong Kong Joint Research Centre for Optical Fibre Sensors, State Key Laboratory of Radio Frequency Heterogeneous Integration, Shenzhen University, Shenzhen 518060, China*

[3]*School of Electronics Science, Northeast Petroleum University, Daqing 163318, China*

[*]Corresponding author: Changrui LIAO E-mail: cliao@szu.edu.cn

Abstract: Benefiting from the great advances of the femtosecond laser two-photon polymerization (TPP) technology, customized microcantilever probes can be accurately 3-dimensional (3D) manufactured at the nanoscale size and thus have exhibited considerable potentials in the fields of microforce, micro-vibration, and microforce sensors. In this work, a controllable microstructured cantilever probe on an optical fiber tip for microforce detection is demonstrated both theoretically and experimentally. The static performances of the probe are firstly investigated based on the finite element method (FEM), which provides the basis for the structural design. The proposed cantilever probe is then 3D printed by means of the TPP technology. The experimental results show that the elastic constant k of the proposed cantilever probe can be actively tuned from 2.46 N/m to 62.35 N/m. The force sensitivity is 2.5 nm/μN, the Q-factor is 368.93, and the detection limit is 57.43 nN. Moreover, the mechanical properties of the cantilever probe can be flexibly adjusted by the geometric configuration of the cantilever. Thus, it has an enormous potential for matching the mechanical properties of biological samples in the direct contact mode.

Keywords: Optical fiber sensor; microforce sensing; microstructured cantilever; two-photon polymerization

Citation: Famei WANG, Changrui LIAO, Mengqiang ZOU, Dejun LIU, Haoqiang HUANG, Chao LIU, *et al.*, "Microstructured Cantilever Probe on Optical Fiber Tip for Microforce Sensor," *Photonic Sensors*, 2024, 14(2): 240204.

1. Introduction

With the trend of device miniaturization, micromanipulation and microforce measurement have attracted great interest from researchers in various fields [1–4]. In the microscopic world, tiny objects are easily damaged by excessive external forces, so reliable and high-precision microforce measurement is of great significance for the biomedicine, microassembly, and equipment protection [5–7]. The design and implementation of the miniaturized and highly sensitive microforce sensor is one of the most important research goals in the field of mechanics. In recent years, optical fiber

Received: 8 August 2023 / Revised version: 23 October 2023

DOI: 10.1007/s13320-024-0704-6
Article type: Regular

microforce sensors based on different fiber structures have been developed, such as the fiber Bragg grating (FBG) [8–10], micro-nano fiber (MNF) [11–13], Fabry Perot interferometer (FPI) [14–17], and Mach Zehnder interferometer (MZI) [18]. Among these microforce sensors, the optical fiber FPI microforce sensor is widely concerned because of its high sensitivity, simple configuration, fast response, and miniaturization.

As an ultra sensitive micro-electro-mechanical system (MEMS) device, the microcantilever has the advantages of non-labeling, real-time, positioning, and specific detection, and has been widely used as the atomic force microscope (AFM) probe and other detection elements [19]. Since the FPI formed between the microcantilever and the end face of the optical fiber can detect the weak vertical deformation of the cantilever, the optical fiber FPI sensor based on the microcantilever has gradually attracted the attention of scientists. Compared with manual alignment integration methods, additive manufacturing selectively adds materials to three-dimensional (3D) structures [20–22]. The micro-nano scale additive manufacturing technology is mainly based on the chemical process of photoresist polymerization and curing. It uses this material to generate and distinguish soluble or insoluble blocks under laser exposure conditions, build preset graphics on the two-dimensional (2D) level, and finally form micro-nano structures through the spatial stacking of materials [23, 24]. The two-photon polymerization (TPP) can directly add materials to print various complex micro-nano structures on the fiber substrate, effectively realize the precise integration of the microcantilever beam and optical fiber, and make it possible to combine the MEMS technology with the optical fiber sensing technology [25–27]. In the previous work, based on most of the research, the structure designed and prepared has always remained in the common rectangular shape [28–30]. Therefore, the flexible design of the cantilever probe structure and the unique mechanical properties of the structure given by 3D printing have not been deeply explored. Up to now, it is still a challenge to realize arbitrarily shaped cantilever probes. Therefore, the force sensor based on the microstructure cantilever beam probe needs further development.

In this paper, a novel microforce sensing technology based on femtosecond laser induced two-photon polymerization for the fabrication of the fiber end for a fiber-optic microforce sensor is proposed. The controllable microstructure of the microcantilever beam endows it with the force sensitivity. Based on the finite element method (FEM), the static performance of the structure is simulated, which provides a basis for the structural design. The elastic constant k of the designed the fiber end for a fiber-optic microforce sensor can be actively adjusted from 2.46 N/m to 62.35 N/m. We can adjust the geometry of the cantilever to change the mechanical properties of the probe to match the mechanical properties of the biological sample. The force sensitivity of this type of optical fiber microforce sensor is 2.5 nm/μN, Q is 368.93, and the detection limit is 57.43 nN. A new and practical optical fiber micro-force sensing technology is realized, which promotes the application of the optical fiber micro-force sensing technology in biomechanics, material science measurement, and other key fields.

2. Sensing principle of the sensor

The complex feedback path of the AFM system is replaced by optical fiber transmission, and the signal is obtained by optical interference. The FP sensor consists of a single-mode optical fiber (SMF) and a micro-cantilever beam, as shown in Fig. 1. The reflectivity spectrum of the sensor consists of three beam interference formed by the optical fiber end face, the lower surface of the cantilever beam, and the upper surface of the cantilever beam. An air microcavity (FPI1) is formed between the end face of the optical fiber and the lower surface of the

microcantilever beam. A polymer microcavity (FPI2) is formed between the upper and lower surfaces of a microcantilever beam. Finally, a hybrid microcavity (FPI3) is formed between the optical fiber end face and the upper surface of the microcantilever beam. Here, the light intensity of FPI3 is relatively weak compared to FPI1 and FPI2, and the light intensity of FPI2 is fixed after the cantilever is manufactured. Therefore, when a force is applied to the probe of a microcantilever beam, the change of the reflection spectrum is caused by the change of FPI1 in the air medium. The free spectral range of FPI1 can be calculated by the following formula [31]:

$$\mathrm{FSR} = \frac{\lambda^2}{2nL} \tag{1}$$

where λ is the resonant wavelength, L is the cavity length of the FP cavity, and n is the refractive index of the cavity medium in the FP cavity.

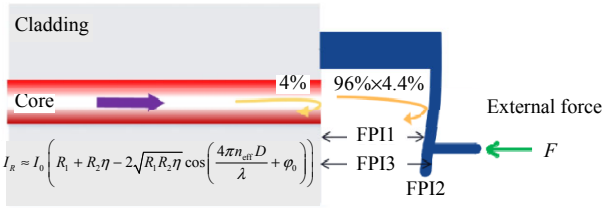

Fig. 1 Schematic diagram of the interference principle for the fiber optic end face FPI.

When the probe is subjected to force, the cantilever is bent and deformed, and the optical path difference and interference fringe of the FP cavity change. The bending degree of the cantilever can be determined by detecting the wavelength of the wave crest or trough in the interference spectrum. The correspondence between the wavelength change ($\Delta\lambda$) and the cavity length of the FP cavity change (ΔL) can be simplified as follows [32]:

$$\frac{\Delta\lambda}{\lambda} = \frac{\Delta L}{L}. \tag{2}$$

By monitoring the drift of the interference spectrum, the variation in the cavity length can be inferred, and then the external force applied to the probe can be measured.

3. Simulation design of the sensor

In order to optimize the sensing characteristics of the fiber end polymer microcantilever microforce sensor, microcantilever beams with different shapes are designed. As we all know, the hollow structure is the best topology covering a 2D plane. Therefore, we select hexagons, circles, and triangles as elements to perform the hollow design on rectangular cantilever beams and optimize their mechanical properties. Under the principle of the control variable method, the details of the microcantilever beam with the hollow structure are completely consistent except that the side length of the cell is different. The base of the cantilever beam is a cuboid with a length of 20 μm, a width of 20 μm, and a height of 40 μm. The total length of the cantilever beam is 60 μm. In addition, a cylindrical probe with a radius of 2 μm and a height of 15 μm is designed at the end of the microcantilever beam. The front end of the cantilever beam is designed as a small area block to improve its deflection sensitivity. The length of a small area block at the front end of the microcantilever beam depends on the diameter of the optical fiber core (about 9 μm) and the error of the printing position. The rectangular block with a length of 15 μm is selected to ensure that the light is fully reflected back into the fiber by the lower surface of the microcantilever. In order to study the static mechanical properties of the proposed hollow structure cantilever probe, we use the COMSOL Multiphysics software to establish force sensor models with different structural parameters under the same stress, and the simulation results are shown in Figs. 2(a)–2(c). The material parameters, Young's modulus, the Poisson ratio, and the density of the polymer cantilever, are set to 2.34 GPa, 0.33, and 1499 $\mathrm{kg \cdot m^{-3}}$, respectively. The physical field of solid mechanics is selected, and the same microforce of 1 μN is applied to the probe. The deformation of each area under the force is shown in Figs. 2(a)–2(c).

The deformation increases with an increase in the side length of the hollow structure cell. The deflection of the microcantilever beam varies with the side length of its hollow structure cell, as shown in Figs. 2(a)–2(c). The reason is that an increase in the side length reduces the effective area of the cantilever beam. The smaller the effective surface area of the cantilever beam is, the larger the flexure deformation is, and the higher the sensitivity of the sensor is.

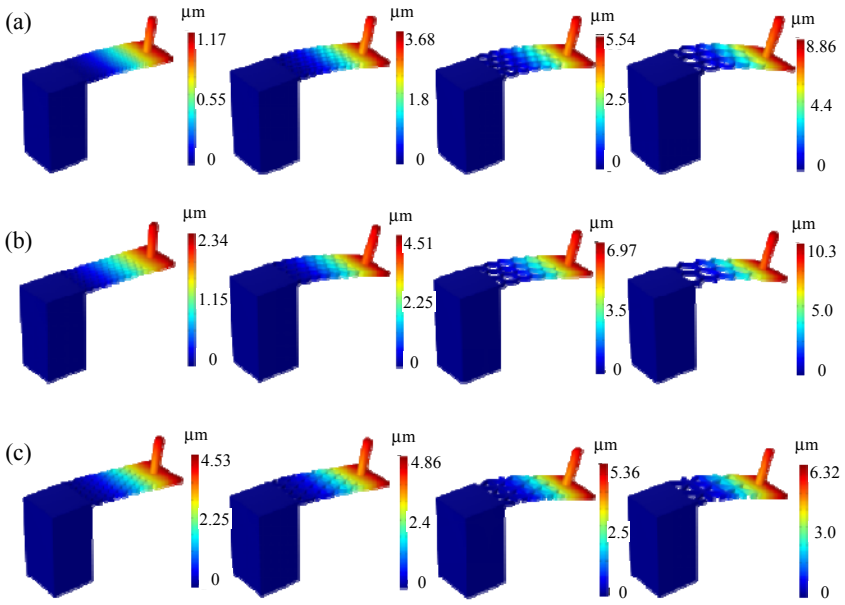

Fig. 2 Simulation results of the deflection distribution with microcantilever beams of different shapes: (a) finite-element analysis on stress distributions of circular structure microcantilever probes with the radius of the circular cell of 1 μm, 2 μm, 3 μm, and 4 μm, respectively, (b) finite element analysis on stress distributions of hexagonal structure microcantilever probes with the side lengths of the hexagonal cell of 2 μm, 3 μm, 4 μm, and 5 μm, respectively, and (c) finite element analysis on stress distributions of triangular structure microcantilever probes with the side lengths of the triangular cell of 4 μm, 6 μm, 8 μm, and 10 μm, respectively.

4. Fabrication and characterization of the sensor

The hollow structure microcantilever probe at the end of the optical fiber is fabricated using the TPP by a femtosecond laser. Here, a drop of photoresist (IP-S) is dripped onto the optical fiber tip to immerse the end face and then transferred to our home-made femtosecond laser-induced TPP equipment. The femtosecond laser power, repetition rate, and central wavelength are 30 mW, 80 MHz, and 800 nm. The laser beam is focused on the sample and the liquid is converted into a solid by polymerization along the path of the focused laser beam in the photoresist. After polymerization, the sample is first immersed in propylene glycol methyl ether acetate (PGMEA) for at least 10 min and then in isopropyl alcohol for approximately 5 min to rinse away any residual photoresist. At the same time, ultraviolet irradiation is performed to provide uniform cross-linking of the printed structure to ensure its mechanical stability. After washing, the cantilever is then printed successfully onto the fiber tip. Figure 3(a) shows the scanning electron microscope (SEM) images of a microcantilever beam. The SEM images in Fig. 3(a) show that the actual size of the microcantilever beam is consistent with the design. It basically consists of three parts. At the bottom, the base support column consists of a cube with a cross-sectional area of 20 μm×20 μm×40 μm. At the top, the microcantilever beam with a beam length of 60 μm, a hollow

structure cell side length of 4 μm, a beam width of 20 μm, and a beam thickness of 4 μm is attached to the support column. At the front end of the cantilever beam, a large area square is used to improve its deflection sensitivity, and a probe with a diameter of 4 μm and a height of 15 μm is attached to the square for force detection. It can be seen from the top view that the surface is smooth and the shape is complete. The rectangular block at the end of the microcantilever blocks the fiber core to stimulate interference.

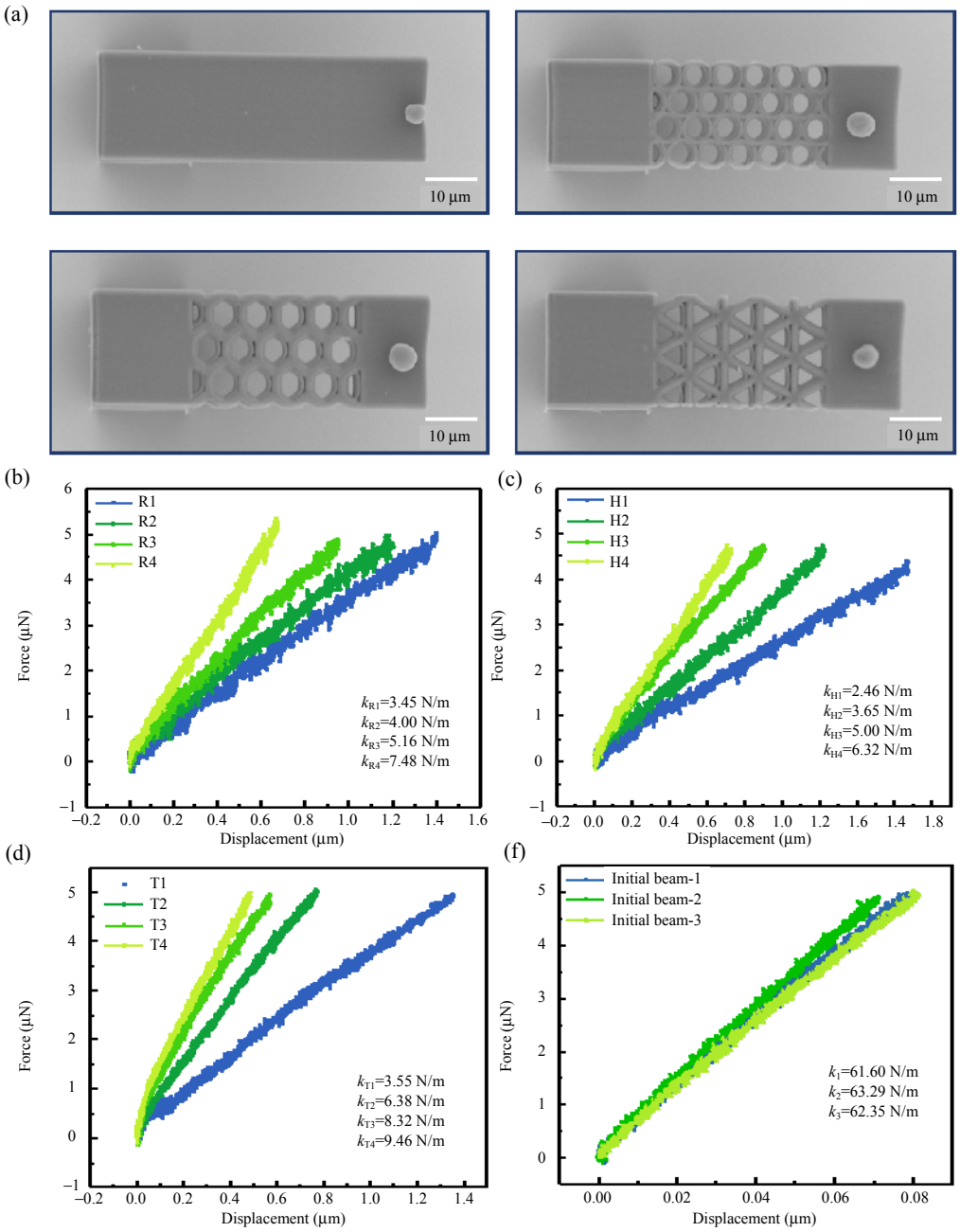

Fig. 3 SEM images and stiffness characteristics with microcantilever beams of different shapes: (a) SEM images of microcantilever beams, (b) force-displacement curves of circular structure microcantilever probes with the radius of the circular cell of 4 μm, 3 μm, 2 μm, and 1 μm, respectively, (c) force-displacement curves of hexagonal structure microcantilever probes with the side lengths of hexagonal cell of 5 μm, 4 μm, 3 μm, and 2 μm, respectively, and (d) force-displacement curves of triangular structure microcantilever probes with the side lengths of the triangular cell of 10 μm, 8 μm, 6 μm, and 4 μm, respectively, and (e) force-displacement curves of three rectangular microcantilever beams.

In order to determine the mechanical properties of the hollow structure microcantilever probe at the end of the optical fiber, all characterizations are performed using a nano-indentation (Hysitron TI980). The hollow structure of the microcantilever is an important factor to determine the performance of the microforce sensor. The size of the periodic porous structure is considered to play an important role in the mechanical performance of the microcantilever. In this section, the influence of the side length of the hollow structure cell on the mechanical properties of the microcantilever structure is studied. At first, the radius of the circular structure cell is increased from 1 μm to 4 μm to examine their overall mechanical performances, as shown in Fig. 3(b). The force curves of four sets of the microcantilever exhibit well-separated lineshapes. In Fig. 3(b), the elastic constant k ranges from 3.45 N/m to 7.48 N/m. It can be seen from Fig. 3(c) that the elastic constant k gradually decreases with an increase in the side length of the hollow structure cell of the microcantilever beam. The further analysis in Fig. 3(c) focuses on the elastic constant k, which ranges from 2.46 N/m to 6.32 N/m. Next, the side length of the triangular structure cell is increased from 4 μm to 10 μm to examine their overall mechanical performances. As shown in Fig. 3(d), the elastic constant k ranges from 3.55 N/m to 9.46 N/m.

The duty cycle of the air holes in three different structures of microcantilever beams is compared in Table 1. It can be seen that the larger the duty cycle of the air holes in microcantilever beams is, the smaller the elastic coefficient k is. Finally, its stability is discussed by measuring three different rectangular microcantilever beams. The experimental results provided in Fig. 3(e) show that the force curves of three rectangular microcantilever beams, and k remains at the same value of (62.35±0.94) N/m. The small fluctuations observed in sensitivity confirm that the structure has the good mechanical stability and repeatability under printing conditions. More importantly, we can change the mechanical properties of the microforce sensor by adjusting the size of the side length of the hollow structure cell so as to match the mechanical properties of the biological sample.

Table 1 Performance comparison of different hollow structure microcantilever beams.

Hollow structure	Size of the side length (μm)	k (N/m)	Duty cycle of the air hole (%)
R4	4	3.45	74.9
R3	3	4.00	73.4
R2	2	5.16	63.0
R1	1	7.48	47.9
H4	5	2.46	79.6
H3	4	3.65	73.8
H2	3	5.00	63.2
H1	2	6.32	54.6
T4	10	3.55	72.1
T3	8	6.38	56.8
T2	6	8.32	44.3
T1	4	9.46	36.6

5. Microforce measurement

Three types of performance analysis of the proposed hollow structure cantilever probe are carried out, namely, elastic properties, optical properties, and mechanical properties. The elastic properties of the proposed hollow structure cantilever probe have been discussed in detail above. Here, we choose the cantilever probe with the elastic coefficient (k=5.00 N/m) to analyze its optical and mechanical properties. The morphology of the sample is characterized by the SEM. Figures 4(a) and 4(b) show a series of SEM images. The hollow structure cantilever probe on the end face of the optical fiber is clearly visible and the morphology is complete. It can be seen that the force sensor is composed of the SMF and hollow structure cantilever beam probe. The hollow structure cantilever probe is composed of three parts. At the bottom, the base support column consists of a cube with a cross-sectional area of 20 μm×20 μm×40 μm. At the top, the microcantilever beam with a beam length of 60 μm, a hollow structure cell side length

of 4 μm, a beam width of 20 μm and a beam thickness of 4 μm is attached to the support column. At the front end of the cantilever beam, a small area rectangular block is used to improve its deflection sensitivity, and a probe with a diameter of 4 μm and a height of 15 μm is attached to the square for force detection. Because of the low stiffness of the polymer material, the thickness of the cantilever beam cannot be too small. So we choose 4 μm to ensure the support and high sensitivity of the cantilever beam. Figures 4(a) and 4(b) show the electron microscope pictures of the microcantilever probe of the hollow structure taken from different angles, showing the relatively smooth surface of the microcantilever and the good parallelism between the optical fiber end face and the microcantilever. These characteristics contribute to improving the intensity of the reflected light and the sensitivity of the device to deformation, which lay an ideal foundation for the sensing spectrum.

According to (2), the micro force sensitivity can be obtained by the tilt wavelength shift caused by the unit force of the hexagonal hollow cantilever probe. The experimental device consists of the broadband light source (BBS), optical spectrum analyzer (OSA), 3 dB coupler, and 3D electric displacement platform for the micromanipulation sensor, as shown in Fig. 4(e). Figure 4(c) shows the reflection spectrum of the microcantilever beams. The interference spectrum shows three-beam interference formed by the resonances of three mirrors on the fiber end face and on the upper and lower surfaces of the microcantilever beam. The small envelope within the spectrum is formed by the FP cavity of the air medium, which contains the deflection information of the microcantilever beam to be monitored. The free spectral range of the microcantilever near the wavelength of 1412.8 nm is 40.8 nm and the extinction ratio is 16.3 dB. According to (1), the cavity length of the prepared microcantilever is approximately 24.5 μm. The error between the measured cavity length and the design height of the sensor base is due to the fact that during the printing process, it approaches the interior of the fiber end face by about 15 μm, preventing the probe from falling off during the development process. Based on the nano-indentation test system, the static mechanical properties and micro-force sensitivity of the cantilever probe with the hollow structure are tested. Firstly, a hexagonal hollow cantilever probe with a spring constant of 5.0 N/m is tested. The cantilever probe is fixed on the Physik Instrumente (PI) piezoelectric displacement table, and the microcantilever probe is gradually pressed into the hard glass substrate with a step length of 164 nm under the drive of the PI piezoelectric displacement table. The indentation depth of the hard glass substrate can be regarded as 0. According to Hooke's law ($F=kd$), the micro force of the cantilever probe is 820 nN per step. During the application of the progressive force, the reflection spectrum is monitored in real time. Figure 4(d) shows the reflection spectrum change of the sensor beam probe when the force gradually increases from 0 to 5.74 μN. The blue shift can be clearly observed at the tilted wavelength, as shown by the arrow. The extinction ratio of the reflection spectrum decreases with an increase in the force due to the bending of the cantilever beam. The relationship between the tilt wavelength and the force is shown in Fig. 4(f). With an increase in the applied force, the falling wavelength moves linearly to the shorter wavelength. By using the linear fitting of the falling wavelength change, the force sensitivity of the force sensor is calculated to be 2.5 nm/μN, which is two orders of magnitude higher than the previously reported optical fiber force sensor. *R*-squared (R^2) describes the matching degree of data and fitting function, which is 0.99269. It is worth noting that in our micro force sensing measurement, the sensor probe works within the framework of the linear elastic range, and there is no lag between the force and the change of the cavity length.

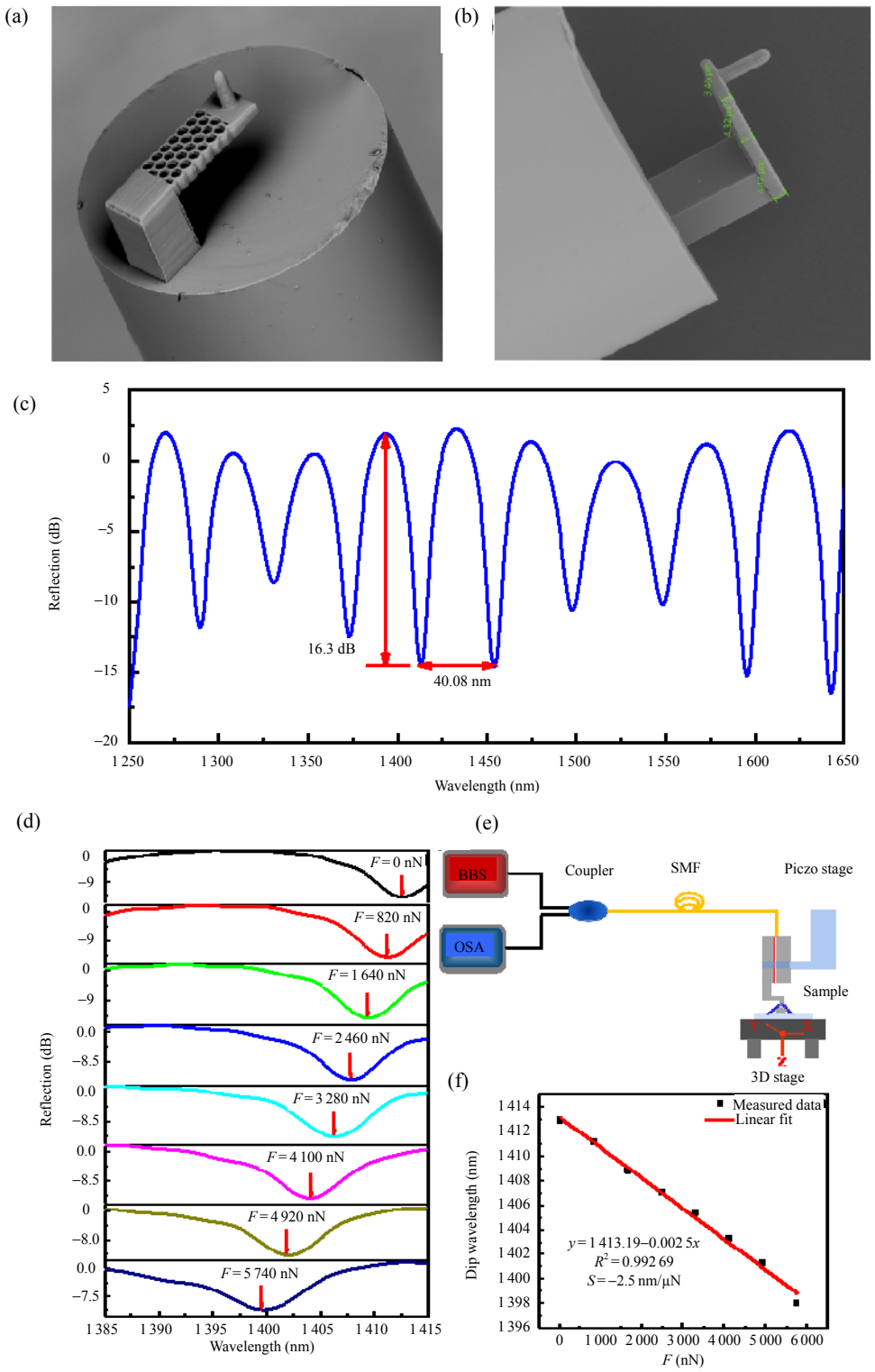

Fig. 4 Experimental setup and microforce measurement: (a) and (b) SEM images of the hexagonal hollow cantilever probe, (c) and (d) reflection spectra of the sensor, (e) measurement system setup, and (f) linear fitting between the spectral variable and the force.

For an ideal sensor device, the Q factor and detection limit (DL) of the sensor are also important, because they represent the overall performance of the system. For optical fiber sensors, Q is defined as follows [33]:

$$Q = \frac{\lambda_Q}{\Delta\lambda_Q} \tag{3}$$

where λ_Q is the central wavelength of the resonant peak, $\Delta\lambda_Q$ is the half peak width of the resonant peak. According to the spectrum of Fig. 4 (c), λ_Q and $\Delta\lambda_Q$ are 1412.98 nm and 3.83 nm, respectively, so Q is 368.93.

The detection limit (DL) is usually determined by the sensor resolution (R) and sensor sensitivity (S). S can be directly obtained from the calculation results. R can be approximately solved by individual noise variances (namely, $R = 3\sigma$) [34]:

$$\mathrm{DL} = \frac{R}{S}. \tag{4}$$

Standard deviation (σ) is used to describe amplitude changes due to the noise, SNR is the signal to noise ratio. At the spectral resolution of the demodulator instrument, σ also exists in spectral changes [35]:

$$\sigma = \frac{\Delta\lambda_Q}{4.5(\mathrm{SNR}^{0.25})}. \tag{5}$$

In our microforce sensing experiment, the main limitation of the DL is $\Delta\lambda_Q$. The measured value of $\Delta\lambda_Q$ is 3.83 nm, and the SNR is expressed in linear units (50 dB). The DL of the device is calculated as 57.43 nN. Such an ultra small DL value can help the proposed sensor detect tiny force changes.

6. Conclusions

This work proposes the design and manufacture of the hollow structure cantilever probe microforce sensor on the end face of an SMF employing a femtosecond laser induced TPP 3D microprinting technology. The elastic constant k of the designed fiber end for a fiber-optic microforce sensor can be actively adjusted from 2.46 N/m to 62.35 N/m. We can adjust the geometry of the cantilever to change the mechanical properties of the probe to match the mechanical properties of the biological sample. The force sensitivity of this type of the optical fiber microforce sensor is 2.5 nm/μN, Q is 368.93, and DL is 57.43 nN. Due to the flexibility and extensibility of polymer materials, the sensor shows the excellent stability and repeatability in multiple mechanical cycles. The sensor has the advantages of the simple manufacture, super high sensitivity, flexibility, and great reproducibility, and has potential application prospects in the field of biomechanical detection.

Acknowledgment

This work was supported by the Shenzhen Science and Technology Program (Grant No. RCYX20200714114524139), Shenzhen Key Laboratory of Ultrafast Laser Micro/Nano Manufacturing (Grant No. ZDSYS20220606100405013), Natural Science Foundation of Guangdong Province (Grant Nos. 2022B1515120061 and 2022A1515110971), National Natural Science Foundation of China (Grant Nos. 62122057, 62075136, 62105217, and 62305223), and China Postdoctoral Science Foundation (Grant No. 2022M722173).

Declarations

Conflict of Interest Yiping WANG is an editorial board member for Photonic Sensors and was not involved in the editorial review, or the decision to publish this article. All authors declare that there are no competing interests.

References

[1] M. Guix, J. Wang, Z. An, G. Adam, and D. J. Cappelleri, "Real-time force-feedback micromanipulation using mobile microrobots with colored fiducials," *IEEE Robotics and Automation Letters*, 2018, 3(4): 3591–3597.

[2] H. Zhang, K. Wang, J. Li, J Li, R. Zhang, and Y. Zheng, "Liquid-based nanogenerator fabricated by a self-assembled fluoroalkyl monolayer with high charge density for energy harvesting," *Matter*, 2022, 5(5): 1466–1480.

[3] Z. Xie, L. Yong, and J. Li, "Development and testing of an integrated smart tool holder for four-component cutting force measurement," *Mechanical Systems & Signal Processing*, 2017, 93: 225–240.

[4] N. Khatibzade, A. B. Stilgoe, A. A. Bui, Y. Rocha, G. M. Cruz, V. Loke, *et al*., "Determination of motility forces on isolated chromosomes with laser tweezers," *Scientific Reports*, 2014, 4(1): 1–9.

[5] M. S. Kim, J. R. Pratt, U. Brand, and C. W. Jones "Report on the first international comparison of small force facilities: a pilot study at the micronewton level," *Metrologia*, 2011, 49(1): 70.

[6] Y. Ota, M. Ueki, and N. Kuramoto, "Evaluation of an automated mass comparator performance for mass calibration of sub-milligram weights," *Measurement*, 2021, 172: 108841.

[7] K. T. Yoon, S. R. Park, and Y. M. Choi, "Electromagnetic force compensation weighing cell with magnetic springs and air bearings," *Measurement Science and Technology*, 2020, 32(1): 015905.

[8] A. Iadicicco, M. D. Pietra, M. Alviggi, and S. Campopiano, "Deflection monitoring method using fiber Bragg gratings applied to tracking particle detectors," *IEEE Photonics Journal*, 2014, 6(6): 1–10.

[9] L. Zhang, Y. Liu, X. Gao, and Z. Xia, "High temperature strain sensor based on a fiber Bragg grating and rhombus metal structure," *Applied Optics*, 2015, 54(28): E109–E112.

[10] R. Li, Y. Chen, Y. Tan, Z. Zhou, T. Li, and J. Mao, "Sensitivity enhancement of FBG-based strain sensor," *Sensors*, 2018, 18(5): 1607.

[11] Y. Chen, S. C. Yan, X. Zheng, F. Xu, and Y. Lu, "A miniature reflective micro-force sensor based on a microfiber coupler," *Optics Express*, 2014, 22(3): 2443–2450.

[12] Q. Huang, J. Lee, F. T. Arce, I. Yoon, P. Angsantikul, and J. Liu, "Nanofibre optic force transducers with sub-piconewton resolution via near-field plasmon-dielectric interactions," *Nature Photonics*, 2017, 11(6): 352–355.

[13] P. Youplao, M. Tasakorn, and T. Phattaraworamet, "The simulation of a force in micro-scale sensing employing an optical double ring resonator system," *Pertanika Journal of Science & Technology*, 2018, 26(1).

[14] Y. Liu, S. Qu, W. Qu, and R. Que, "A Fabry-Pérot cuboid cavity across the fibre for high-sensitivity strain force sensing," *Journal of Optics*, 2014, 16(10): 105401.

[15] Y. Wu, S. Xiao, Y. Xu, Y. Shen, Y. Jiang, W. Jin, *et al*., "Highly sensitive force sensor based on balloon-like interferometer," *Optics & Laser Technology*, 2018, 103: 17–21.

[16] S. Pevec and D. Donlagic, "Miniature all-fiber force sensor," *Optics Letters*, 2020, 45(18): 5093–5096.

[17] W. Bao, X. Li, F. Chen, R. Wang, X. Qiao, "Hyperelastic polymer fiber Fabry-Pérot interferometer for nanoforce measurement," *Journal of Lightwave Technology*, 2022, 40(12): 4020–4026.

[18] C. Liao, D. Wang, and Y. Wang, "Microfiber in-line Mach-Zehnder interferometer for strain sensing," *Optics Letters*, 2013, 38(5): 757–759.

[19] A. Sierakowski, D. Kopiec, W. Majstrzyk, P. Kunicki, P. Janus, R. Dobrowolski, *et al*., "Magnetoelectric versus thermal actuation characteristics of shear force AFM probes with piezoresistive detection," *Measurement Science and Technology*, 2017, 28(3): 034011.

[20] Q. S. Sun, Z. X. Xue, Y. Chen, R. Xia, J. Wang, S. Xu, *et al*., "Modulation of the thermal transport of micro-structured materials from 3D printing," *International Journal of Extreme Manufacturing*, 2022, 4: 015001.

[21] M. Q. Zou, C. R. Liao, S. Liu, C. Xiong, C. Zhao, J. Zhao, *et al*., "Fiber-tip polymer clamped-beam probe for high-sensitivity nanoforce measurements," *Light: Science & Applications*, 2021, 10(171): 2047–7538.

[22] C. R. Liao, C. Xiong, J. L. Zhao, M. Zou, Y. Zhao, B. Li, *et al*., "Design and realization of 3D printed fiber-tip microcantilever probes applied to hydrogen sensing," *Light: Advanced Manufacturing*, 2022, 3(1): 3–13.

[23] I. Sakellari, S. Droulias, A. Lemonis, and E. I. Stratakis, "Femtosecond-laser-induced all-silicon dielectric metasurfaces assisted by wet chemical etching," *Ultrafast Science*, 2023, 3: 0019.

[24] X. Chen and M. Gu, "Two-beam ultrafast laser scribing of graphene patterns with 90-nm subdiffraction feature size," *Ultrafast Science*, 2022, 2022: 0001.

[25] J. H. Strickler and W. W. Webb, "Three-dimensional optical data storage in refractive media by two-photon point excitation," *Optics Letters*, 1991, 16(22): 1780.

[26] M. H. Wang, K. H. Zhao, J. Y. Wu, Y. Li, Y. Yang, S. Huang, *et al*., "Femtosecond laser fabrication of

nanograting-based distributed fiber sensors for extreme environmental applications," *International Journal of Extreme Manufacturing*, 2021, 3(2): 025401.

[27] M. Malinauskas, A. Žukauskas, V. Purlys, K. Belazaras, A. Momot, D. Paipulas, *et al*., "Femtosecond laser polymerization of hybrid/ integrated micro-optical elements and their characterization," *Journal of Optics*, 2010, 12(12): 124010.

[28] M. Q. Zou, C. R. Liao, Y. P. Chen, L. Xu, S. Tang, G. Xu, *et al*., "3D printed fiber-optic nanomechanical bioprobe," *International Journal of Extreme Manufacturing*, 2023, 5(1): 015005.

[29] C. Xiong, C. R. Liao, Z. Y. Li, M. Zhu, Y. Zhao, Y. Wang, "Optical fiber integrated functional micro-/nanostructure induced by two-photon polymerization," *Frontiers in Materials*, 2020, 7: 586496.

[30] M. Q. Zou, C. R. Liao, Y. P. Chen, Z. Gan, S. Liu, D. Liu, *et al.*, "Measurement of interfacial adhesion force with a 3D-printed fiber-tip microforce sensor," *Biosensors*, 2022, 12(8): 629.

[31] C. P. Lang, J. D. Zhu, Y. Liu, Y. Li, and S. Qu, "Ultra compact full-angle-range direction-distinguishable tilt sensor based on fiber in-line polymer microcavity," *Journal of Lightwave Technology*, 2022, 40(9): 3084–3089.

[32] M. Li, Y. Liu, X. L. Zhao, S. Qu, and Y. Li, "Miniature Pi-shaped polymer fiber tip for simultaneous measurement of the liquid refractive index and temperature with high sensitivities," *Journal of Optics*, 2015, 17(10): 105701.

[33] P. Ji, M. Zhu, C. R. Liao, C. Zhao, K. Yang, C. Xiong, *et al*., "In-fiber polymer microdisk resonator and its sensing applications of temperature and humidity," *ACS Applied Materials & Interfaces*, 2021, 13(40): 48119–48126.

[34] C. X. Li, Y. Liu, C. Lang, Y. Zhang, and S. Qu, "Femtosecond laser direct writing of a 3D microcantilever on the tip of an optical fiber sensor for on-chip optofluidic sensing," *Lab on a Chip*, 2022, 22(19): 3734–3743.

[35] I. M. White and X. D. Fan, "On the performance quantification of resonant refractive index sensors," *Optics Express*, 2008, 16(2): 1020–1028.